11-9-2023

Electro-cementation of calcareous sand using colloidal silica (CS) nanoparticles and alumina powder

Nermeen Fouad Ashour

Ashraf Kamal Hussein

Rami Mahmoud El Sherbeeny

Omar Osman Omar

Recommended Citation

APA Citation
Ashour, N. Hussein, A. El Sherbeeny, R. & Omar, O. (2023). Electro-cementation of calcareous sand using colloidal silica (CS) nanoparticles and alumina powder. *Innovative Infrastructure Solutions, 8*, 10.1007/s41062-023-01276-6
https://fount.aucegypt.edu/faculty_journal_articles/5214

MLA Citation
Ashour, Nermeen Fouad, et al. "Electro-cementation of calcareous sand using colloidal silica (CS) nanoparticles and alumina powder." *Innovative Infrastructure Solutions,* vol. 8, 2023,
https://fount.aucegypt.edu/faculty_journal_articles/5214

TECHNICAL PAPER

Electro-cementation of calcareous sand using colloidal silica (CS) nanoparticles and alumina powder

Nermeen Fouad Ashour[1] · Ashraf Kamal Hussein[2] · Rami Mahmoud El Sherbeeny[2] · Omar Osman Omar[3] · Safwan Abbas Khedr[4]

Abstract

The research investigates the effectiveness of a ground improvement technique that involves the electro-cementation of an onshore calcareous sand containing 95.3% calcium carbonate through a series of laboratory experiments. Colloidal silica (CS) nanoparticles and alumina powder were introduced as pozzolanic materials in the sand, and a direct current (DC) was passed through the sand-silica-alumina mix inside an electrokinetic (EK) cell. The method resulted in the electro-cementation of the calcareous sand through the formation of calcium silicate hydrates (C–S–Hs) and calcium aluminate hydrates (C–A–Hs) as products of the pozzolanic reactions between $Ca(OH)_2$, SiO_2 and Al_2O_3 after electrolysis occurred. Iron-rich cements were also formed by the degradation of anodes. These newly formed compounds changed the nature of the treated soil from a granular material into a rock. Results show that the compressive strength of the resulting rock formation is significantly improved. The treatment can be considered as an artificial lithification process through which the nature of the treated soil was changed from a granular material into a rock formation. The electro-cementation achieved by the treatment was further assessed by spectroscopic analyses including FE-SEM, EDX and XRD, which confirmed the formation of cementing agents within the structure of the treated sand. Potential applications of the technique include caissons, highway construction projects, dune fixation and erosion control, in addition to liquefaction mitigation due to electrolysis of pore water and plugging the pores with cementitious materials.

✉ Safwan Abbas Khedr
safkhedr@aucegypt.edu

Nermeen Fouad Ashour
nermeen.ashour@aucegypt.edu

Ashraf Kamal Hussein
Mr.ashrafkh07@gmail.com

Rami Mahmoud El Sherbeeny
rsherbiny@gmail.com

Omar Osman Omar
ootg64@yahoo.com

[1] Faculty of Engineering, Cairo University, Giza, Egypt

[2] Soil Mechanics and Foundations Division, Faculty of Engineering, Cairo University, Giza, Egypt

[3] Highway, Traffic, and Airport Engineering Department, Giza, Egypt

[4] Construction Engineering Department, The American University in Cairo, Cairo, Egypt

Introduction

Calcareous sediments are sediments with more than 30% calcium carbonate mainly precipitated by weathering of highly carbonate rocks and/or biological processes by marine organisms. The particle size of calcareous sediments varies from sand to clay sizes, although most are sand to silt sized. Calcareous sand is a problematic type of soil due to its high void ratios, irregular particle shape, high compressibility and crushability. It mainly consists of calcareous bioclastic remains. These fragmented bones by nature have microintra- and interpores leading to the characteristic porosity of the calcareous sand [1]. The intrapores result in high crushability and consequently low load-carrying capacity [2]. Calcareous sand is considerably more compressible than silica sand [3]. It can sometimes be 30 times more compressible than quarzitic sands under the same loading conditions and stress levels [4].

Calcareous sand covers approximately 50% of the sea-floor on Earth with predominance in tropical and subtropical regions [5]. It covers a large percent of the north coastal region of Africa. Calcareous sand in Egypt forms the sand dunes of the Mediterranean coastal line. The $CaCO_3$ content in the calcareous sand of Egypt reaches 99%, ranked the highest percentage worldwide, followed by the calcareous sand dunes of Australia, Iran, Mexico and the United Arab Emirates, with 90%, 90%, 76% and 70% $CaCO_3$, respectively.

The increase in population and the subsequent urbanization have led to the inevitable need for the construction on problematic soils such as calcareous sand. Accordingly, geotechnical engineers are often challenged to come up with unconventional technologies and innovative materials in the field of ground improvement to overcome geotechnical challenges and at the same time conform to environmental sustainability standards which have become one of the world's foremost goals. Therefore, engineers should make conscious selection of materials and construction methods based on sustainability aspects. Traditional stabilisation materials used in ground improvement, including cement and chemical stabilisers such as synthetic polymers have negative environmental impacts, in addition to their limitations in non-disruptive field treatments. The manufacturing industry of cement alone emits 8-10% of the global CO_2 emissions. This is because the production of 1 ton of cement results in 1 ton of CO_2 being released into the atmosphere [6]. Cement also has a high pH value, which can be a problem when a controlled and stable environment is needed. In recent years, nanomaterials have attracted many researchers in the field of civil engineering [7]. Introducing nanomaterials as new soil stabilisation materials is an important step towards green and sustainable construction. Among the nanomaterials used in soil stabilisation is colloidal silica (CS). And while calcium carbonate is very well known to treat siliceous sands, much less is known about the effect of silica on the behaviour of calcareous sands. Therefore, this research adopts a novel ideology for the stabilisation of calcareous sand; an obscure soil, using CS; a new-level nanomaterial. There are limited studies on CS as a grout material for soil stabilisation used mostly in siliceous sands. But, to the best of our knowledge, none of the exiting studies has adopted the ideology of adding CS as a pozzolanic material to the calcareous sand and testing the outcomes of their chemical reaction after electrolysis occurs in an electrokinetic process.

Electrokinetic stabilisation is a promising ground improvement technique that enhances the engineering behaviour of weak soils by injecting chemical stabilisers into the soil through an electrokinetic treatment. It was pioneered by Casagrande in the late 1940s on soft soils and since then it has been mostly used and studied for fine-grained soils [8]. The treatment mechanism of electrokinetic stabilisation techniques is the hybrid effect of electroosmosis and electromigration. The first is the movement of water and the latter is the movement of ions in the soil by applying a DC current through the soil matrix. It has been implemented successfully in geotechnical engineering applications and has shown to bring about improvement in the geotechnical properties of weak soils including the increase of the shear and compressive strengths [9]. Electrokinetic stabilisation can be more effective than other conventional ground improvement techniques. Although it has the potential to be more widely used, and although much research has been conducted, the field applications of the electrokinetic stabilisation technique are still very limited [8, 9]. This is because the technique relies on many factors, some of which are related to the soil type, some to the electrodes and others to external surrounding conditions. All these factors are site-specific, which makes it difficult to have a standardised procedure or frame for the process.

As mentioned earlier, the technique has been studied and implemented mainly on soft soils, rather than granular soils. Very few exceptional small bench-scale studies are currently present on offshore calcareous sand. And while a vast variety of chemical stabilisers are studied and well-known for ground improvement techniques such as chemical grouting, only a few types of soils and chemical stabilisers are found in the literature on EK treatment.

The electrochemical cementation of offshore calcareous sand was studied through a laboratory-floor experimental study by [10]. A caisson, 200 mm in diameter and 400 mm long, was embedded in calcareous sand under seawater. Twelve electrodes were installed around the caisson and were filled with soluble $CaCl_2$ granules as a cementing agent. An electric current was passed over a period of 7 days. Current intermittence and polarity reversal were applied. The efficiency of the treatment was assessed by a pullout test. The caisson was then pushed back into the soil, and the treatment was repeated to simulate post-failure recovery. Results showed that the pullout resistance of the foundation model increased by 140% and 255% prior to failure and post-failure, respectively, compared to that of the control test. In a study conducted by [11], the effect of the electric field intensity on electro-cementation of offshore calcareous sand was investigated via large-scale model tests and electric field analyses. Model caissons were embedded in the calcareous sand with a central electrode placed inside the caisson and a DC intermittent electric current was applied for a period of 7 days. Shear wave measurements were used to monitor the development of cementation in the treated calcareous sand during electrokinetic treatment. As a result of the electrokinetic treatment, the pullout resistances of the caisson model were found to increase up to 105%. The effect of electrode configuration on electrokinetic stabilisation for caisson anchors in offshore calcareous sand was

studied by [12] through a series of large-scale laboratory tests on caisson models of 200 mm in diameter and 400 mm long, embedded in calcareous sand submerged under seawater. Two-electrode configurations were investigated, 12 electrode poles surrounding the caisson and a central electrode extended below the base of the caisson. The results suggested that the central electrode should be positioned below the caisson, with minimal overlap inside the caisson to maximize the effectiveness of the EK treatment. Electric field analysis was also carried out to verify the results. It was found that the effectiveness of the EK treatment is directly proportional to the electric field intensity and can be optimised by increasing the electric field intensity surrounding the caisson and by decreasing the electric field intensity inside the caisson. Also, a linear relationship was observed between the increase in the side resistance of the caisson models and energy consumption. The EK treatment resulted in significant iron-rich cements and increased the pullout resistance of the caissons by over 90%. A feasibility study of the coupled effect of hydraulic and electrophoretic injecting of CS grout in loose sand was conducted by [13]. The results showed that electrophoretic injection of CS could be useful to stabilize the loose sand. And that, throughout the injection of the grout, electrophoretic injection accelerated gelation compared to the hydraulic injection alone. A study by [14] also investigated the effect of coupled electric and hydraulic flow in CS injection in a sandy soil, in which grouts with 10% and 30% by weight CS were injected under an electric gradient of 1.5 V/cm and 2 V/cm, respectively. Results showed that the electrokinetic effect is stronger than a hydraulic flow with a 1.15 hydraulic gradient.

This research investigates the effectiveness of treating calcareous sand using the single effect of CS nanoparticles and the binary effect of CS and Al_2O_3 powder, as pozzolanic materials, in an electrokinetic process. The objectives of the research are to study the potential use of electro-cementation of calcareous sand using CS nanoparticles and alumina powder, to test the soil's mechanical properties by determining the increase in the compressive strength of the treated calcareous sand after electro-cementation is induced by the proposed method and to investigate the mineralogical changes after the treatment.

Mechanism of the treatment

Electrokinetic stabilisation is a ground improvement method that has been employed for dewatering, consolidation, stabilisation and contaminant removal of crystalline minerals in soils. It is a physicochemical transport of charge in which ions migrate within the soil mass towards the electrode of the opposite charge, resulting in changes in soil pH. This transport occurs due to electrolysis reactions. These reactions alter the soil's chemical composition and cause mineral formation.

Electrokinetic stabilisation includes four main transport mechanisms within the soil mass: electroosmosis, electrolysis, electrophoresis and electromigration. Electroosmosis is the movement of pore water through the soil from the anode to the cathode. Electrophoresis is the movement of charged particles, including colloids and organic particles, causing sedimentation [8]. Electromigration is the movement of ions in a soil due to an applied electric field. The ions move towards the electrode of opposite charge, anions towards the anode and cations towards the cathode. Among the four movement types, electromigration is the most important transport mechanism in electrokinetic stabilisation [15].

Chemistry of the process

The proposed treatment in the current study induces electrochemical reactions that generate electro-cementation. The electric current obtained from the power supply is used to force the chemicals in the electrolytic cell to undergo chemical reactions after their electrolysis takes place. Hardening of the treated soil is achieved at both the anode and the cathode because of ion migration and exchange leading to the formation of new minerals (mineralisation) and their precipitation inside the soil mass.
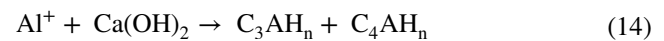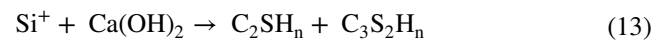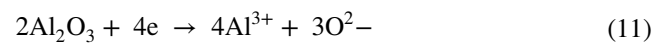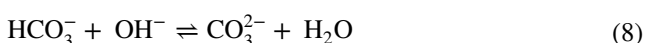
Passing an electric current causes metal degradation of the anode. As a result, metal atoms are lost from the surface of the anode and deposited into the sand in the form of metal cations, as shown in Eq. 1. Electrolysis of H_2O takes place in the Ek cell, as shown in Eqs. 2 and 3. Positively charged hydrogen ions and negatively charged hydroxyl ions migrate to the electrode of opposite charge. Ferrous ions migrate towards the cathode and react with hydroxyl groups to give ferrous hydroxide $[Fe(OH)_2]$, as shown in Eq. 4. Moreover, further oxidation and the precipitation of ferric ions (Fe^{3+}) lead to the formation of ferrihydrite ($Fe(OH)_3 \cdot nH_2O$), as shown in Eq. 5, resulting in more iron-rich cements within the treated sand. Precipitated ferric oxyhydroxide minerals include maghemite $\gamma\text{-}Fe_2O_3$, hematite $\alpha\text{-}Fe_2O_3$, lepidocrocite $\gamma\text{-}FeOOH$ and goethite $\alpha\text{-}FeOOH$. These minerals are all originally ferrihydrite (rust) which is $Fe(OH)_3 \cdot nH_2O$, a metastable amorphous compound formed in the cathodic region.
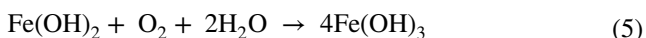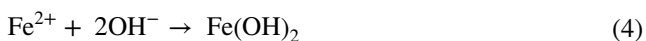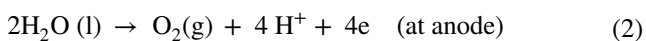
On the other hand, electrolysis of $CaCO_3$ takes place in the EK cell and Ca^{2+} ions are freed, as shown in Eq. 6. The resulting metal cation Ca^{2+} and carbonate anion CO_3^{2-} migrate to the electrode of opposite charge, forming $Ca(OH)_2$ at the cathode and carbonic acid (H_2CO_3) at the anode, respectively. The electrolysis of calcium carbonate is a greener alternative to its calcination during cement manufacture. Calcination is the thermal decomposition of $CaCO_3$ which results in the

conversion of carbonates to oxides, forming CaO. This takes place at extremely high temperatures, making the process a major contributor to CO_2 emissions, whereas electrolysis is the ionic dissociation of $CaCO_3$ separating the cation (Ca^{2+}) part of the compound from the anion part ($CO_3)^{2-}$. Carbon dioxide that results from the electrolysis reaction dissolves in water between pH values 8 and 10, forming dissolved carbonic acid, as shown in Eqs. 7 and 8. This disposal of CO_2 makes the treatment have a low carbon footprint. Ferrous ions (Fe^{2+}) which are precipitated in the sand mix react with the carbonate anions $(CO_3)^{2-}$ to form the mineral siderite ($FeCO_3$), as shown in Eq. 9.

Simultaneously, the electrolysis of SiO_2 and Al_2O_3 occurs, as shown in Eqs. 10 and 11. Ion migrations of free and ready-to-react Ca^{2+}, Si^+, Al^{2+}, CO_3^{2-} and OH^- towards the electrode of opposite charge take place. Reaction between Ca^{2+} metal cation and OH^- group takes place giving slaked lime $Ca(OH)_2$, as shown in Eq. 12. The formation of slaked lime is necessary for the formation of cementitious materials. Pozzolanic reactions between $Ca(OH)_2$ and reactive silica and alumina in the presence of water at ambient temperature lead to the formation of C–S–H and C–A–H gels, respectively, as shown in Eqs. 13 and 14. These gels fill the pores of the treated sand and bond the particles together.

Crystallisation and recrystallisation of the newly formed cementitious materials bring about more hardening to the treated sand. The EK treatment lasted 7 days. After the completion of the EK treatment, the treated sand was left inside the EK cell for 60 days before sample extraction. Although the current ceased, the pozzolanic activity continues beyond the treatment time.

$$Fe \rightarrow Fe^{2+} + 2e \tag{1}$$

$$2H_2O\ (l) \rightarrow O_2(g) + 4\ H^+ + 4e \quad \text{(at anode)} \tag{2}$$

$$2H_2O(l) + 2e \rightarrow H_2(g) + 2OH^-(aq) \quad \text{(at cathode)} \tag{3}$$

$$Fe^{2+} + 2OH^- \rightarrow Fe(OH)_2 \tag{4}$$

$$Fe(OH)_2 + O_2 + 2H_2O \rightarrow 4Fe(OH)_3 \tag{5}$$

$$\left[\text{Ferrihydrite} \left(Fe(OH)_3 . nH_2O \right) \right]$$

$$CaCO_3 + 4e \rightarrow Ca^{2+} + CO_2 + \tfrac{1}{2}\ O_2 \tag{6}$$

$$CO_2 + H_2O \rightarrow H_2CO_3 \tag{7}$$

$$HCO_3^- + OH^- \rightleftharpoons CO_3^{2-} + H_2O \tag{8}$$

$$Fe^{2+} + CO_3^{2-} \rightarrow FeCO_3 \downarrow \tag{9}$$

$$SiO_2 + 4e \rightarrow Si^+ + 2O_2 \tag{10}$$

$$2Al_2O_3 + 4e \rightarrow 4Al^{3+} + 3O^{2-} \tag{11}$$

$$Ca^{2+} + (OH)^- \rightarrow Ca(OH)_2 \tag{12}$$

$$Si^+ + Ca(OH)_2 \rightarrow C_2SH_n + C_3S_2H_n \tag{13}$$

$$Al^+ + Ca(OH)_2 \rightarrow C_3AH_n + C_4AH_n \tag{14}$$
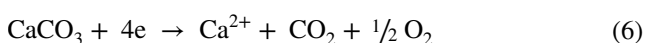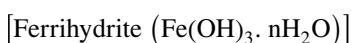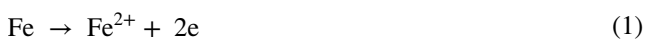
Soil pH and buffering capacity

Soil pH is a key factor in any EK treatment. Electro-cementation generated by the EK treatment is primarily governed by water pH which, in turn, is controlled by the soil pH and acid buffering capacity. And hence, alteration in the microstructure of the treated soil mainly depends on soil pH. Ionic diffusion and, thus, mineralisation are directly proportional to the pH. Pozzolanic reactions take place in alkaline mediums between pH 9 and 12. Alkalinity increases the cation exchange capacity, resulting in higher dissolution of minerals and thus in more C–S–H and C–A–H formations. It was reported by several references in the literature that at pH 9–10, the dissolution of silicate and aluminate is optimised. This explains why mineral formation, hardening and strength gain are more pronounced at the cathode rather than at the anode. If the soil has a low buffering capacity, electrode polarisation occurs at the interface between the metallic and the ionic conductors, in other words between the electrode and the electrolyte [16]. Electrode polarisation is due to water electrolysis when the two constituents of a water molecule do not move at the same speed in the electrolyte solution, but rather at different rates of advection. During electromigration, positive hydrogen ions possess a faster ionic mobility due to a higher ratio of charge to ionic size. Hydroxyl groups $(OH)^-$ are generated near the cathode and move towards the anode, increasing the pH of the soil and preventing an acid front from building up near the anode, and by that, promotes the precipitation of pore fluid, resulting in the strengthening of the soil. However, hydroxyl groups $(OH)^-$ move towards the anode much slower than hydrogen ions (H^+) due to the relatively large size of the hydroxyl ions. This causes an acidic front to develop in the soil near the anode causing the development of an isolating barrier at the interface between the electrode and the electrolyte solution and hence affects the efficiency of the EK treatment. When polarisation occurs during the treatment, the

process becomes detrimental to the electrodes and adversely affects the efficiency of EK treatments [16]. Therefore, in EK treatments intended for ion precipitation and cementation, soils with low acid buffering capacity may require the application of anode depolarisation technique among the commonly used techniques used to increase the efficiency of EK treatments. The anode depolarisation technique is the prevention of the development of such barriers by creating an alkaline environment at the anode.

Among the factors promoting the suitability of calcareous sand for EK treatment is the absence of organic matter. Organic matter consumes OH^- ions and reduces oxidation, which are crucial for the success of the treatment to produce cementation. More importantly, calcareous sand has a dominating alkaline nature due to its chemical composition and the presence of the carbonate anion in its main component ($CaCO_3$). This prevents a highly acidic environment from building up inside the EK cell and promotes pozzolanic activity. According to XRF analysis, the calcareous sand used in this study contains 95.34% $CaCO_3$ and thus anode depolarisation was not required in the EK treatment. The high buffering capacity of the calcareous sand and its ability to withstand the pH fluctuations arising from the EK process prevented an acidic front from developing near the anode by hindering the H^+ ions from migrating into the soil and at the same time enabling the OH^- ions to migrate towards the anode.

## Materials used

Calcareous sand

Calcareous sand used in this study was obtained from a site 300 km northwest of Cairo and 30 km east of Al Dabaa. The sand particles show variation in shape from rounded to subrounded and subangular. The colour of the particles varies from light tan to white. Individual particles are characterised by having rough surfaces.

Chemical composition of calcareous sand

Chemical characterisation and elemental analysis of calcareous sand were carried out using X-ray fluorescence (XRF) and energy-dispersive X-ray (EDX) tests, respectively. The analyses showed that the calcareous sand samples have 95.34% calcium carbonate content and traces of quartz and other minerals and ions. The chemical composition using XRF analysis of the untreated calcareous sand is indicated in Table 1. Figure 1 shows the EDX analysis for untreated calcareous sand.

Table 1 XRF analysis of untreated calcareous sand

Minerals/Ions	%
SiO_2	0.3
TiO_2	–
Al_2O_3	0.23
Fe_2O_3	0.07
MgO	0.98
CaO	53.39
Na_2O	0.34
K_2O	0.33
MnO	–
Cl^-	0.12
P_2O_5	0.09
SO_3^-	0.36
Ca_2CO_3	95.34
Loss on ignition	43.7
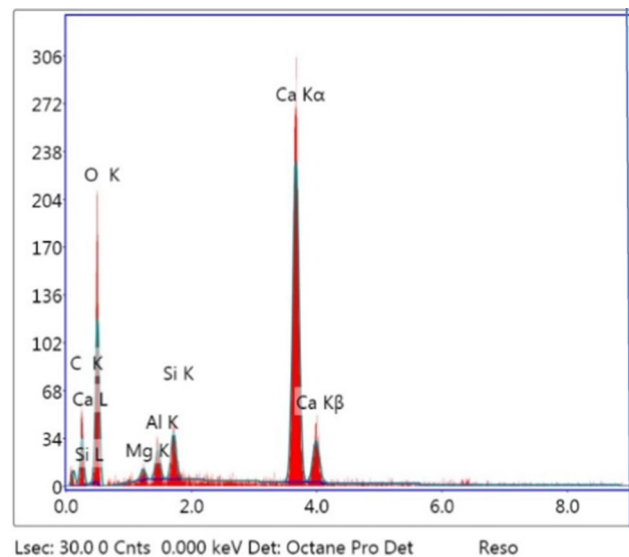
Fig. 1 Energy-dispersive X-ray (EDX) of untreated calcareous sand

Geotechnical characterisation of calcareous sand

The grain size distribution was determined in general accordance with [17]. The coefficient of uniformity, Cu, and the coefficient of curvature, Cc, determined from the results of the particle size analysis were 1.4 and 1.03, respectively. The maximum and minimum void ratios for the calcareous sand are 1.045 and 0.752, respectively. The sand is classified as calcite sand according to [18]. Figure 2 shows the gradation curve of the calcareous sand. The sand is poorly graded sand with silt (SP-SM) according to the Unified Soil Classification System (USCS) with a specific gravity of 2.74. Modified Proctor compaction test was conducted on the calcareous sand according to [19]. The compaction test results show that the maximum dry unit weight for the

Fig. 2 Grain size distribution curve for untreated calcareous sand
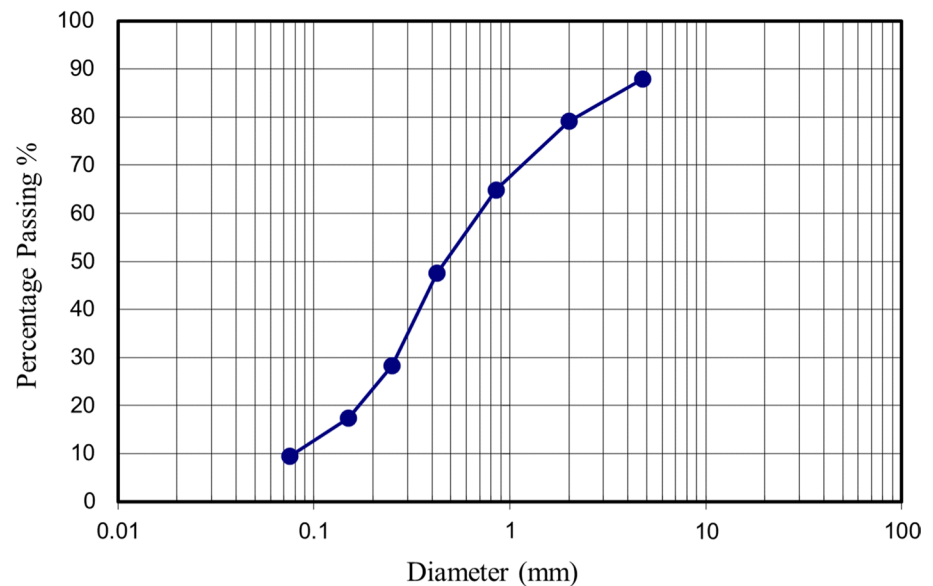
calcareous sand is 2.07 gm/cm^3 and the optimum moisture content is 8%.

Colloidal silica

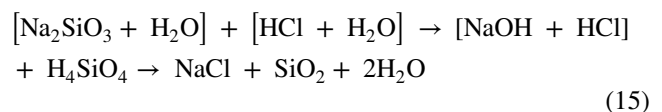Colloidal silica (CS) is a special form of nanosilica, where the nanoparticles are dispersed uniformly, and the initial particle size is maintained. These properties enable CS to perform better as a nanomaterial [20]. It is non-toxic and biologically inert [21].

CS is among the four typical nanomaterials that have been applied to soils for ground improvement. The other three are carbon nanotubes, bentonite and laponite [22]. Among all nanoparticles, CS is advantageous with regard to its characteristics and performance. This is attributed to its high pozzolanic activity due to the presence of high amount of pure amorphous SiO_2 [7], resulting in high chemical reactivity. In addition to its pozzolanic activity, CS has a filling effect. Furthermore, CS is advantageous over the other nanomaterials, with respect to their level of disturbance, environmental friendliness and price/performance ratio [22]. Studies have shown that CS can effectively enhance the shearing resistance of siliceous sand. CS improves shear strength during cyclic loading, in which the treated samples experience very little strain during cyclic loading and remain intact. The unconfined compressive strength of siliceous sand treated with CS increases linearly with increasing the percentage of CS.

As a pozzolan, CS has been used in concrete to replace cement in the mix to improve the strength and durability of the cementitious materials [23]. Silica nanoparticles improve morphology and mineralogy of the cementitious materials by acting as centres of crystallisation, in addition to its filler effect due to the small particle size and large surface area [24].

CS used in this study was synthesised by acidifying low-cost water glass (sodium silicate) with a 12M HCl solution and adjusting the pH at 7 in an acid-base neutralization reaction. Using sodium silicate as the raw material is reported in the literature to have several benefits such as low cost, slow growth rate, dense particles as well as the possibility for particle surface modification [25]. The water glass was diluted with distilled water with a ratio of 2:1. Diluting the water glass with pure water is reported by [23] to produce silica nanoparticles with a small volume mean diameter and a narrow particle size distribution. The aim of using a low-cost starting material was to produce large amounts of nano-sized silica and to allow for mass production to make the proposed treatment feasible on a field scale in ground improvement projects. The chemical reaction for CS synthesis is expressed in Eq. 15.

$$\left[Na_2SiO_3 + H_2O\right] + \left[HCl + H_2O\right] \rightarrow \left[NaOH + HCl\right] + H_4SiO_4 \rightarrow NaCl + SiO_2 + 2H_2O$$

$$(15)$$

The synthesis produced amorphous SiO_2 nanoparticles with specific surface area of 26 m^2/gm and particle size $\cong$ 30 nm. EDX analysis excluded the presence of any impurities in the produced SiO_2. Index properties of CS used in the study are given in Table 2. Transmission electron microscopy (TEM) images of the CS nanoparticles are shown in Fig. 3.

Table 2 Index properties of CS

Index property	Content
Zeta potential	− 44.1 mV
Conductivity	1.38 mS/cm
Refractive index	1.59
Average particle size	30 nm
pH range	6–8
Viscosity	0.8872 cP
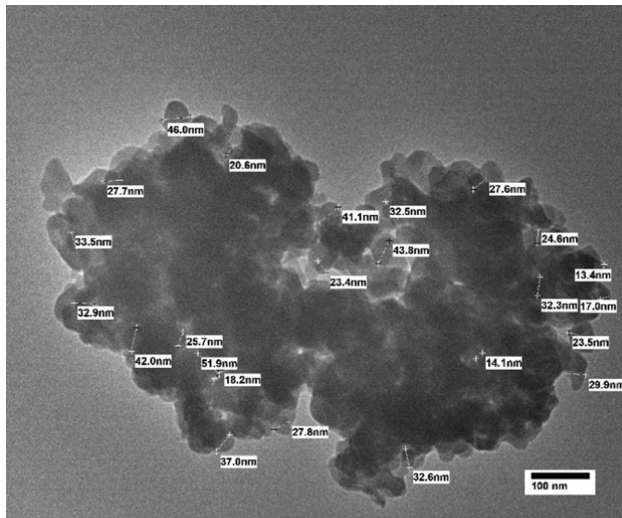
Fig. 3 TEM images for CS nanoparticles

Table 3 Index properties of alumina powder

Property	Value
ASSAY	NLT 98%
pH aqueous solution 5%	6–7.5
Particle size	Passes 175 MESH
Water-soluble matter	0.25%
Loss on ignition	4%

Alumina powder

The alumina powder used in this study is ADVENT aluminium oxide neutral, 175 mesh (88 μm). The role of alumina is to act as an activator which promotes the pozzolanic reaction in addition to its filler effect. Through pozzolanic reactions with $Ca(OH)_2$, the Al_2O_3 particles form C–S–As within the mass of the treated sand. The alumina was added as 1% by weight of sand in T7 and T8. The index properties of the alumina powder are given in Table 3.

Table 4 Summary of treatments

EK treatment	Percent weight(s) of chemical stabiliser(s)	Electrodes
T1	–	Double S.S plate electrodes
T2	10% CS	Double S.S plate electrodes
T3	15% CS	Double S.S plate electrodes
T4	20% CS	Double S.S plate electrodes
T5	20% CS	Double iron plate electrodes
T6	25% CS	Double S.S plate electrodes
T7	10% CS + 1% Al_2O_3	Double S.S plate electrodes
T8	20% CS + 1% Al_2O_3	Double S.S plate electrodes

Experimental work

A series of laboratory experiments were conducted to investigate the effectiveness of the treatment method and to verify the electro-cementation induced by the treatment. Eight treatment tests were conducted using different percentage weights of CS as summarised in Table 4. Alumina powder was added as 1% weight of sand in the presence of 10% CS and 20% CS in T7 and T8, respectively. Double stainless-steel plate electrodes were used in all treatments except in T5 in which double iron plate electrodes were used.

Test setup

Experiments were conducted in eight identical electrolytic (EK) cells. Each cell is a 40-cm-wide, 60-cm-long and 15-cm-high acrylic tank with an open top to avoid pressure build up and to allow gases evolving at the anode and the cathode to escape. The acrylic used was 7 mm thick to resist potential distortion due to high temperatures generated by the electrokinetic process. Figure 4 shows the Ek cell during and after the EK treatment.

Mixing

CS nanoparticles and alumina powder were added to calcareous sand passing sieve #4 (4.75 mm) as percentage weights of the sand, as shown in Table 4. CS was added as 10%, 15%, 20% and 25% weight of the treated sand in treatments T2, T3, T4 and T6, respectively. Alumina powder was added as 1% weight of the calcareous sand in each of the treatments T7 and T8.

For low initial conductivity soils, such as calcareous sand, addition of salt solutions is required for the transfer of the electric current between the soil particles. For this study, brines were made from distilled water and NaCl powder. The CS-sand mix was mixed with 0.6 M NaCl solution to serve
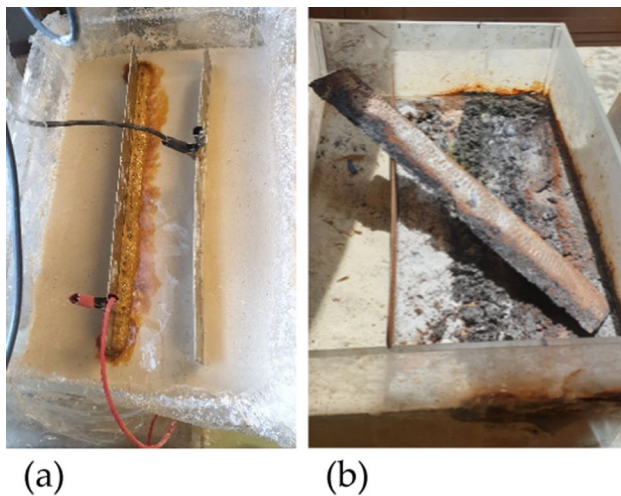
Fig. 4 EK cell **a** at the start of the EK treatment and **b** after the treatment

as an aqueous electrolyte. The electrical conductivity of the NaCl solution used in this study was 5.5 S/m. The initial water content at the start of the EK treatment was 25%.

Uniform mixing of the stabilising agents was ensured by mixing them with the sand inside a concrete drum-type mixer. The pre-designed amount of salt solution was added gradually to the mixture in the drum mixer to ensure homogeneous mixing. The EK cell was then filled with the sand mix and placed on an electric shaker (vibrating table machine) to prevent the presence of air pockets in the sand. This is to avoid the formation of gaps or crevices within the mass of the rock formation resulting from the treatment, which would affect the results of the compressive strength testing. The double-plate electrodes were then inserted into the sand-CS/CS-alumina mix.

Electrodes

Electrode material

Electrode material is one of the major factors affecting the efficiency of any EK treatment. First and foremost, its choice is important because the metal ions of the electrode will diffuse in the soil, form new minerals and become part of the new chemical composition of the treated soil. Second, the rate of corrosion is a function of the electrode potential. Third, the cost of the electrodes is an important element to be taken into consideration for the feasibility of the treatment on a field scale, especially in large-scale projects. It is therefore of great importance to choose the electrode material in view of all the above-mentioned aspects. Candidate metal electrodes commonly used in EK treatments of soils include copper, aluminium, iron and stainless steel. In addition to being relatively expensive, copper electrodes cause

soil contamination and are not environmentally friendly. Aluminium, on the other hand, has the advantage of a relatively low cost. However, although it is a very reactive metal, it is known to become very passive over time. This contradictory nature is plausible because when aluminium is oxidised, it forms a permanent passive aluminium oxide layer which prevents it from further reaction with the surrounding environment. Iron oxides, on the other hand, are known to be cementing agents by nature. They act as catalysts in redox reactions in the EK cell resulting in higher efficiency of the EK treatment. These reactions contribute to electrochemical hardening. The precipitation of iron oxides in the soil forms iron-rich cements, bringing about strength gain. Therefore, the use of iron/steel electrodes serves the objective of the current research which is to induce cementation in the treated calcareous sand.

In the presented study, double stainless-steel electrodes were used in all treatments except in T5, in which double iron electrodes were used to compare the efficiency of the treatment for the same percent weight of CS.

Electrode shape and configuration

In a pilot experiment, double-perforated cylindrical stainless-steel electrodes were used as the anode and the cathode. Each cylinder had an inner diameter of 2.5 cm and was 25 cm long. The perforation holes were 2.5 mm in diameter. Electrode to electrode spacing was 20 cm centre to centre. The effect of EK treatment was found to be confined to the perimeters of the electrodes. Another alternative was to use multiple cylindrical electrodes to spread the mineral formation throughout the entire area of the EK cell. However, fewer samples would be extracted from the EK cell after the removal of the electrodes in such case, in addition to a more complex distribution of mineral formation due to overlapping between anodic and cathodic regions. Therefore, it was decided to use double-plate electrodes instead of cylindrical electrodes in all treatments. The aim was to induce cementation in a more uniform manner within the treated sand sample and to extend the zone of treatment along the whole area of the EK cell. The plate electrodes used in all the treatments were 50 cm long, 25 cm wide, with a thickness of 1.5 mm. Electrode to electrode spacing was 13.3 cm in all treatments. The double-plate electrodes were connected to the power supply via crocodile clip cables.

Power supply, current and applied voltage

A step-down single-phase 220-V power transformer, designed and manufactured for the study, with multi-outputs (12, 24, 36 and 48 V) with a total power of 2 KVA and a maximum rating of 41.6 A was used as a power supply. A bridge full-wave rectifier with a maximum rating of 50 A

was used to convert AC to DC. Capacitors were used for the smoothing of the DC signal obtained from the full-wave rectifier to get a pure DC current. The current intensity was monitored using a current meter connected to the power transformer-bridge rectifier system.

The current intensity was initially high at the beginning of the treatment. Gradual and slight increase in the current took place at the start of the process due to the high concentration of ions and their electromigration in the electrolyte solution. The current then started to decline. This decline happens upon reaching ionic equilibrium due to reduction in the concentration of mobile ions when the ions have reacted to form new compounds in the electrolyte solution [26]. The water content decreased gradually due to evaporation arising from the heat generated by the EK treatment and due to water electrolysis. The decrease in water content over time caused the current intensity to decrease at constant voltage. At the same time, the soil resistivity arising from electrochemical changes within the soil mass caused the current to gradually decrease. The change of soil resistivity over time is due to electro-chemical changes such as ion polarisation in the soil pore fluid. The increases in soil resistivity with time are referred to as resistance polarisation [26]. As the soil resistivity increases with time, the current decreases under constant voltage. This means the current intensity becomes function in time under constant voltage [12]. Figure 5 shows the variation in current intensity with time at a constant voltage of 24 V. In a study by [27], it was stated that, similarly, if a constant current is applied, the corresponding applied voltage will increase. According to the same reference, another study assessed the difference between constant voltage and constant current and found that there was no distinction between the two methods with respect to the properties of the treated soil. In this study, the multi-outputs of the power transformer were used to keep the current constant by increasing the applied voltage.
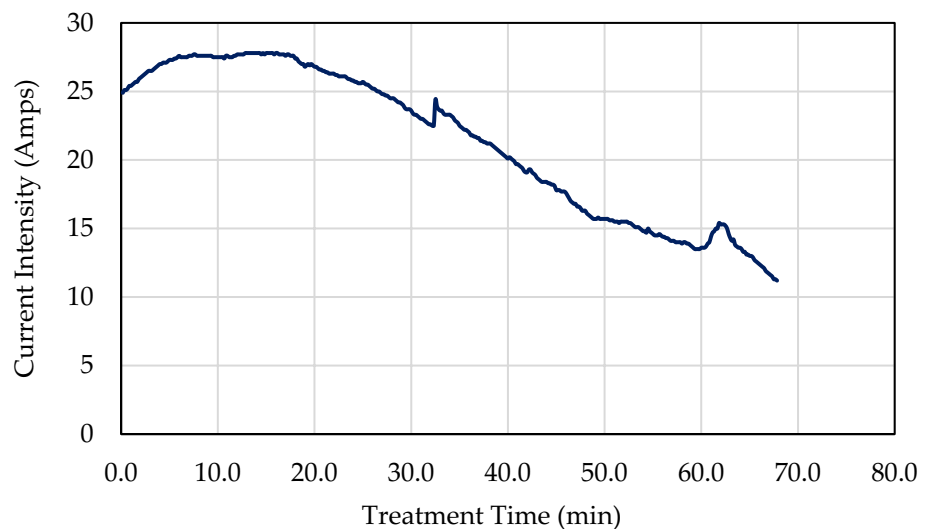
Current intermittence, regular or irregular, has been reported to reduce the rate of anode corrosion and power consumption [28]. In the presented study, current intermittence was not applied; however, the current was turned off at weekends. This means the electricity was applied for five days, turned off for 65 hours and then reconnected for another two days.

Sample extraction and preparation

Post-treatment, pump pincers and sledgehammers were used as aiding tools in the gripping, dislocation and pull out of the cathode. Rock samples were extracted from the EK cell for subsequent mechanical and spectroscopic analyses. Cubic samples for unconfined compressive strength testing were cut using an electric table saw machine, as shown in Fig. 6. Although static compression tests on cubic samples render compressive strength only and not the unconfined shear strength as well, as in the case of cylindrical samples, cubic samples were used in testing for the practicality of sample extraction and preparation. Extraction of cylindrical samples with the commonly used height-to-diameter aspect ratio of 2 to 2.5 was extremely difficult despite using core drill machines of variable powers and core diameters. The cubic samples were 5x5x5 cm.

Samples for compressive strength testing were extracted from the region in the EK cell where hardening was mostly achieved, specifically from the centreline along the length of the EK cell to the cathode plate. Electro-cementation produces a material that is heterogeneous to a large extent. The samples adjacent to the anode can be visually differentiated from those in the middle region between the anode and the cathode and from those adjacent to the cathode, as shown in Fig. 7a. Moreover, heterogeneity is found within the same sample, as shown in Fig. 7b. This is due to the fluctuations in pH and ionic concentrations during the EK process. In

Fig. 5 Variation in current intensity with time at constant voltage = 24 V
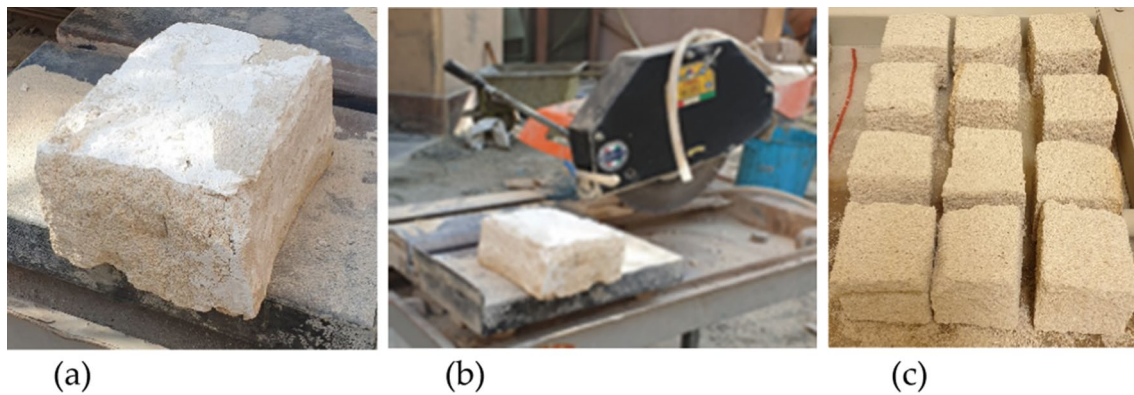
Fig. 6 Preparation of cubic samples for compressive strength testing **a** sample extracted from the EK cell, **b** sample cutting using the electric table saw machine, **c** cubic samples for UCS testing

addition to the fact that corrosion itself is heterogeneous in nature. Mineral formation and thus cementation are more observed at the cathode. Consequently, samples adjacent to the cathode experienced the most profound strength gain. This is because the alkalinity at the cathode is the required medium for pozzolanic reactions to take place and hence for hardening of the treated sample to be achieved. And although corrosion takes place at the anode where electrode metal is degraded, mineral formation takes place at the cathode. This is because metal cations diffuse into the electrolyte and start migrating towards the cathode, reacting with hydroxyl groups to form ferric oxyhydroxide minerals which precipitate near the cathode.

Unconfined compressive strength (UCS) test results

Time-independent static laterally unconfined uniaxial compressive strength tests were performed on cubic samples of the resulting rock formation from each treatment. Strains were measured by measuring displacements, and

stress–strain curves were used to determine the secant modulus of elasticity (E_{50}) taken at a stress level equal to one-half the ultimate compressive strength of the tested rock sample.
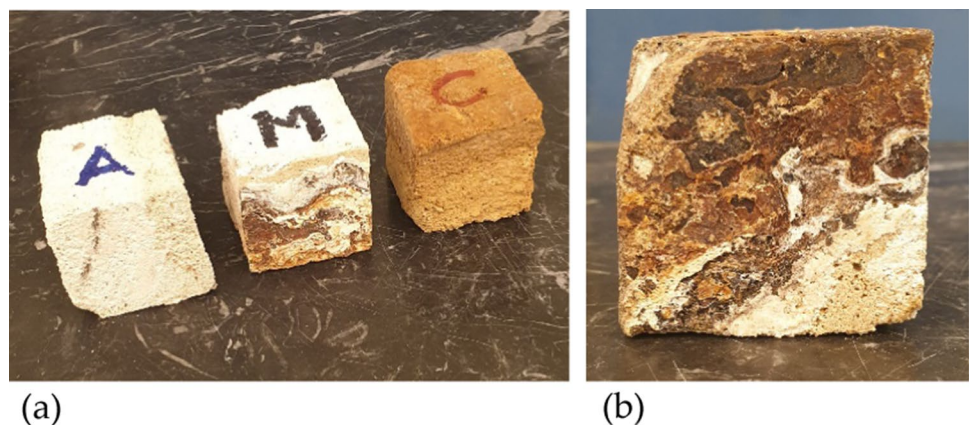
Compressive strength results and Young's modulus of elasticity (E_{50}) for the different treatments are presented in Figs. 8 and 9, respectively.

Analysis and discussion

Results show that the application of a DC current along the calcareous sand sample in the presence of pozzolanic material(s) brought about significant improvement in the compressive strength of the treated sand. The treatment can be considered an artificial lithification process through which the nature of the treated soil was changed from a granular material into a rock formation whose chemical structure is similar to that of artificial siliceous limestone.

The stiffness of the resulting rock formation, reflected by Hook's coefficient of proportionality, showed variability ranging between 25 MPa and 107 MPa. This indicates

Fig. 7 Heterogeneity pronounced in samples **a** from different positions within the EK cell and **b** within the same sample

Fig. 8 Uniaxial compressive strength (σ_{ult}) [MPa] for different treatments
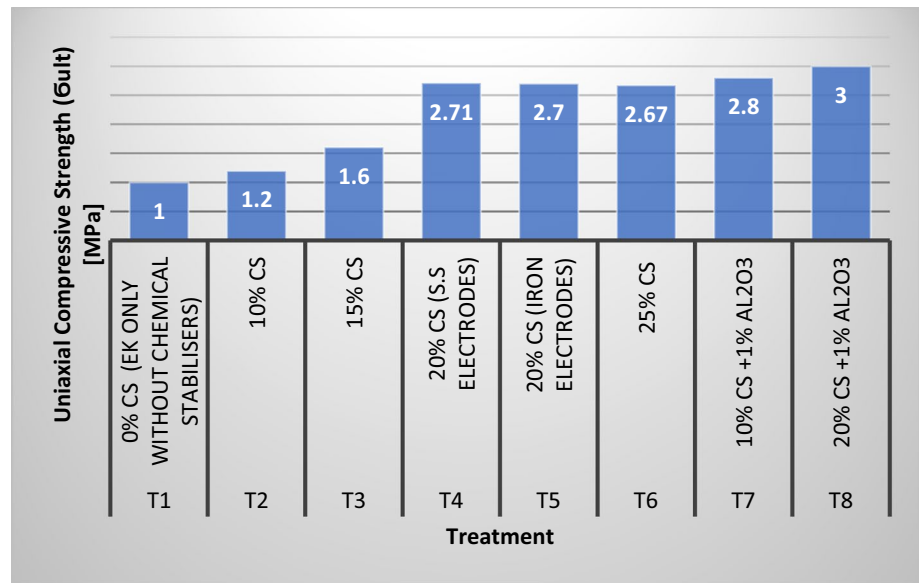
Fig. 9 Young's modulus of elasticity (E_{50}) [MPa] for different treatments

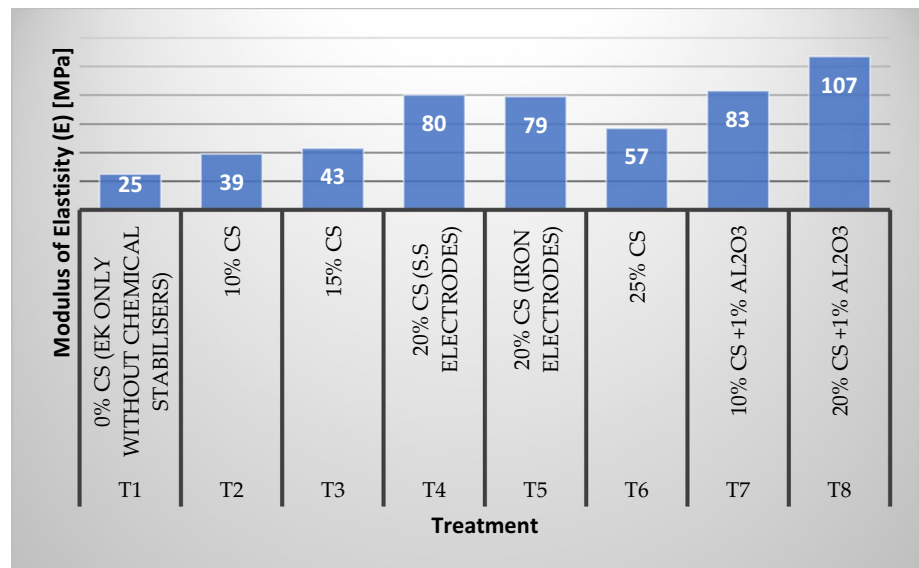that the treatment produced a material whose engineering behaviour varies by varying the amount of chemical stabiliser (CS) and whether the synergistic effect of the two stabilisers (CS and alumina) is in action or not.

Classification of the resulting rock based on compressive strength results

Although tensile and shear strength are very important engineering parameters in the practice of rock mechanics, rock is rarely classified by its tensile strength and never by its shear strength. Instead, it is generally classified based on its compressive strength [29]. And with reference to its compressive strength, the classification is based on two engineering properties: the uniaxial compressive strength and the modulus ratio (M_R) [30]. The modulus ratio is given by Eq. 16.

$$M_R = E_{50}/\sigma_{ult} \tag{16}$$

where E_{50} is the secant modulus at 50% ultimate compressive strength of the rock and σ_{ult} is the uniaxial ultimate compressive strength.

According to this classification, if $\sigma_{ult} < 4000$ psi (27.6 MPa) and $M_R < 200$, as in the present case, then the rock is class *E* which is very low strength and class *L* which is low, based on strength and modulus ratio, respectively [30]. Therefore, the resulting rock formation in the current study, classified both by strength and modulus ratio, is EL.

And according to [29] and [31], the compressive strength range for weak rocks is 1–20 MPa. The rock formation resulting from the proposed treatment in the present study is therefore classified as weak rock. And although compressive strength of 1 MPa is on the weak end of the scale of rock strength, it is not insignificant for engineering design [29].

Factors affecting the results of compressive strength

The compressive strength results are largely affected by the percent weight of CS, the presence of alumina powder in the mix and saturation with water, whereas the effect of electrode material is negligible, as will be discussed in the following subsections.

The effect of CS nanoparticles

The addition of CS nanoparticles significantly enhanced the compressive strength of the treated calcareous sand. Taking T1 as a baseline treatment for comparison, in which the strength gain was due to the electrokinetic treatment only without adding any chemical stabilisers, we find that the compressive strength is enhanced by 20%, 60%, 171% and 167% due to the addition of 10%, 15%, 20% and 25% by weight CS in treatments T2, T3, T4 and T6, respectively. The strength gain was due to the formations of C–S–Hs within the treated sand through pozzolanic reactions between CS and $Ca(OH)_2$. The cementitious materials bonded the sand grains together, increasing its UCS. As a pozzolan, CS further enhanced the morphology and mineralogy of the cemented sand by acting as centres of crystallisation. In addition, the filler effect due to the small particle size and large surface area filled the voids between sand grains. Figure 10 shows the trend of increase in compressive strength with the addition of CS.

There exists a linear relationship between the UCS and the percent weight of CS, in which they are directly proportional. However, the percent increase in compressive strength declines by a fraction from 2.71 to 2.67 MPa upon the addition of 25% CS instead of 20%. This indicates that the optimum percent weight of CS lies between 20% and 25%. It is worth mentioning here that the typical percent weight of SiO_2 in the chemical composition of ordinary Portland cement is reported by [32] as 20%. Additional Si is reported to hinder the crystal growth and prolong strength development, according to [33].
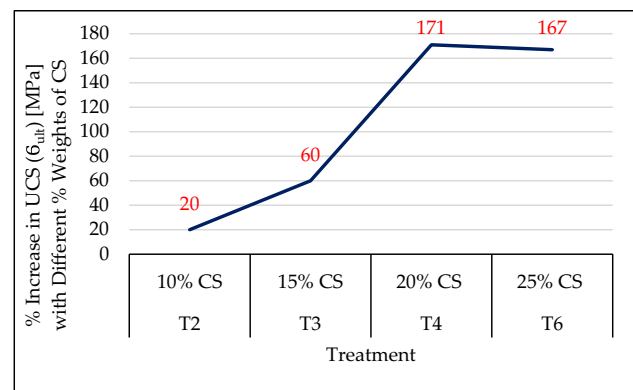

Fig. 10 Percent increase in UCS with the addition of different percent weights of CS compared to baseline treatment T1

The effect of alumina powder

Alumina is one of the most common types of additives used in cementitious composites [7]. Along with iron oxide, aluminium oxide is well known to increase the rate of the reactions, and by that, acts as a mineraliser. The addition of alumina powder to the treated calcareous sand-silica mixes significantly increased the compressive strength of the mix.

Comparing T4 (20% CS) with T7 (10% CS with 1% Al_2O_3), we find that the two treatments yielded very close results of UCS equal to 2.71 MPa and 3 MPa, for T4 and T7, respectively. Similarly, the modulus of elasticity is 80 MPa and 83 MPa, for T4 and T7, respectively. This implies that the compressive strength gain due to the addition of 1% alumina in the presence of 10% CS is equivalent to or even exceeding that brought about by the addition of 20% CS alone. We can then conclude that the incorporation of 1% Al_2O_3 is almost equivalent to the incorporation of 10% CS. Nevertheless, the hybrid effect of the two pozzolans together should not be neglected. Nanosilica is known to accelerate the pozzolanic reactions of other pozzolans. For example, research has shown that pozzolanic activity increases when fly ash and nano-silica were used together than when fly ash and nanosilica were used separately [23].

On the other hand, although T8 (20% CS with 1% Al_2O_3) yielded the best results among all eight treatments with the highest USC, however comparing it with T4 (20% CS only), we notice that the difference in UCS is minor. The unconfined compressive strength and the modulus of elasticity increased by 11% and 34%, respectively, in T8. Whereas comparing T7 (10% CS with 1% Al_2O_3) with T2 (10% CS only), we notice that UCS and E_{50} increased significantly by 133% and 113%, respectively, in T7. Also, if we compare T7 (10% CS with 1% Al_2O_3) with T8 (20% CS with 1% Al_2O_3), the unconfined compressive strength and the modulus of elasticity increased by only 7% and 29%, respectively, in T8, whereas, comparing T2 (10% CS only) with T4 (20%
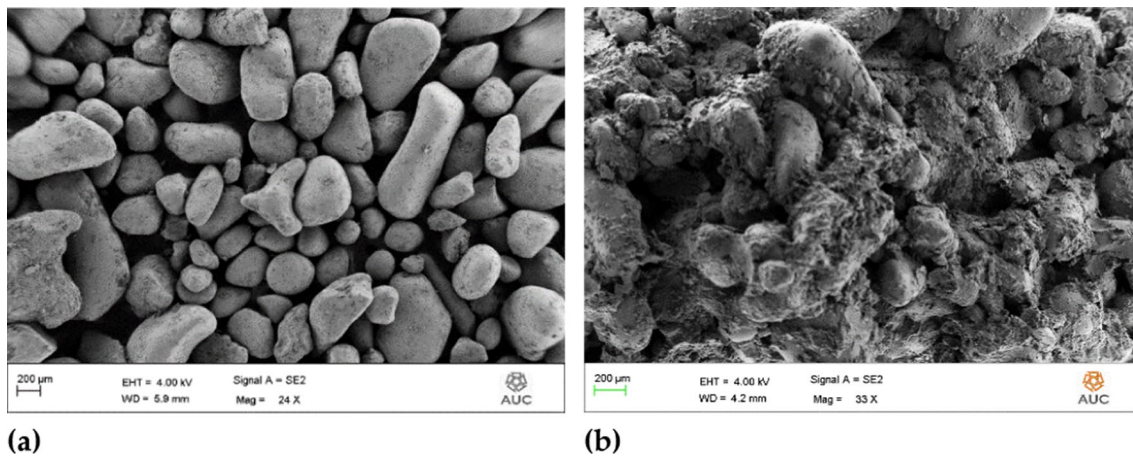
(a)

(b)

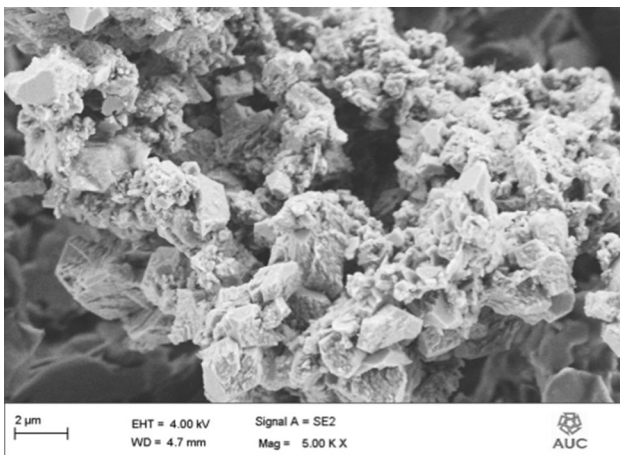**Fig. 11** SEM images of calcareous sand **a** before and **b** after treatment

Fig. 12 SEM image of iron-rich cements formed within treated sand samples from T1

CS only), the unconfined compressive strength and the modulus of elasticity increased significantly by 126% and 105%, respectively, in T4. Interpretation of these observations can be that there was not enough alumina powder to act as an activator for such an amount of CS nanoparticles in T8. In other words, the synergistic interaction was not put to effect in T8. And hence it can be concluded that the increase in compressive strength due to the binary effect of the two additives is largely dependent on their proportionality in the mix.

The effect of electrode material

As mentioned earlier, double stainless-steel plate electrodes were used in all treatment except in T5. In T5, double iron plate electrodes were used to compare the results with those obtained from using stainless-steel plate electrodes at the same percent weight of CS (20%). The findings of the study show that there is no significant difference in the treatment results with using iron than with using stainless-steel plate electrodes. The UCS was 2.71 MPa and 2.7 MPa for T4 and T5, respectively. Young's modulus of elasticity was 80 MPa and 79 MPa for T4 and T5, respectively. The percent increase in compressive strength, compared to the baseline treatment T1, was 171% and 170% for T4 and T5, respectively. Nevertheless, using iron is better from an economic point of view, especially at a field-scale project, as the price of stainless steel is fourfold to fivefold more.

The effect of saturation with water (softening factor)

Water in rock mechanics is known to affect its compressive strength and its elastic properties. Saturated rocks render less values of compressive strength tests than dry ones. This is because the pore water is unable to escape within the limited time of the test, and hence pore water pressure develops as the axial load on the rock sample is increased.

A softening factor (S_f) defines the ratio of dry to wet strength of a rock, as expressed in Eq. 17.

$$S_f = \sigma_{ult}\text{dry avg}/\sigma_{ult}\text{wet avg} \tag{17}$$

Treated samples from T1 and T4 were soaked in water for a 24-h period and then tested in unconfined compressive strength test. The results were 0.3 MPa and 0.95 MPa for T1 and T4, respectively. The value of the softening factor (S_f) is 3.33 and 2.85 for T1 and T4, respectively. These results show that the values of unconfined compressive strength decreased to one-third upon soaking, which conform to the results obtained in a study conducted by [30] on New Jersey Triassic shale in which there was a great and consistent decrease in unconfined compressive strength of the shale
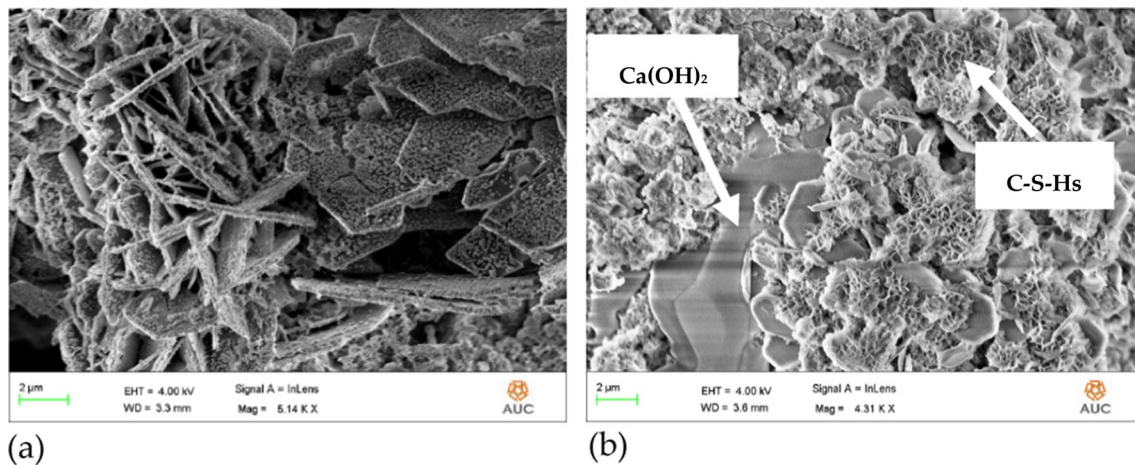
Fig. 13 SEM image displaying **a** hexagonal plates of Portlandite [$Ca(OH)_2$] and **b** C–S–Hs formed within the treated sand samples from T4
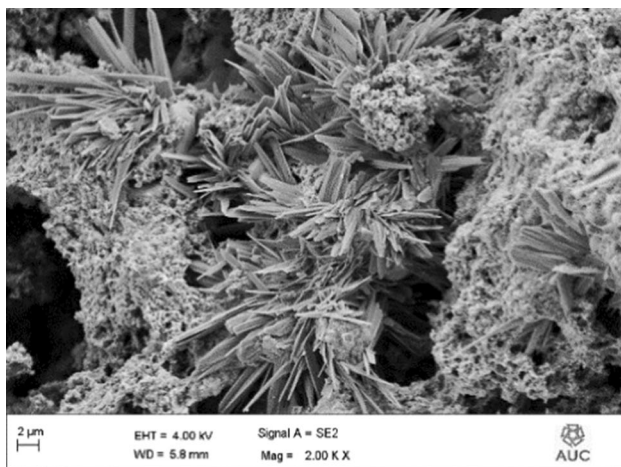
Fig. 14 Self-oriented rosettes of C–S–Hs grown in treated sand samples from T5 (iron electrodes)

specimens upon soaking and the softening factor (S_f) of dry to wet strength was reported to be 3.36.

Spectroscopic analyses for treated sand

Spectroscopic analyses were carried out using field emission scanning electron microscopic imaging (FE-SEM), energy-dispersive X-ray (EDX) and (EDX) mapping and X-ray diffraction (XRD) tests to compare samples of the calcareous sand before and after the EK treatments with respect to the change in soil fabric and the cementation brought about by electromigration, ion precipitation and pozzolanic activity. Results obtained from mineralogical and microstructural tests were used to explain the strength development which relates to the microstructure of the soil and the achieved cementation.

Morphology of the crystals of the cementitious materials formed within the treated sand was observed by high-resolution field emission scanning electron microscope (FE SEM), which enabled the detection and the identification of the crystallographic structure of the newly formed minerals. The images confirmed the cementation of the treated sand and the formation of C–S–Hs and C-A-Hs as well as iron-rich cements, which are not found in the original sand. Figure 11 shows the SEM images of calcareous sand before and after the treatment. The virgin calcareous sand grains contained minute holes on their surface, as shown in Fig. 11a. After treatment, cementitious materials filled these holes and the interparticle voids and joined the particles together in an intact way, as shown in Fig. 11b.

EDX analysis of untreated sand showed peaks of Ca, O and C, but no significant Si or Al was observed, whereas EDX analyses of treated samples showed peaks of Si, Al, Fe, Cr, Ni, Mg, Na and Cl, in addition to the elements originally present in the virgin sand. EDX mapping showed considerable heterogeneity of the samples with respect to the concentration of elements within the same sample but at different points. This heterogeneity is the result of fluctuations in ionic concentrations during EK treatments, as discussed earlier.

XRD analysis confirmed the formation of goethite [α-FeO(OH)] which indicates the oxidation state change of Fe^{2+} (ferrous) to Fe^{3+} (ferric). Iron oxides resulting from the degradation of the anode formed the ferrite phase, which reacted with silicates and aluminates. Iron-rich cements were formed within the microstructure of the treated sand in all treatments and were detected by FE SEM. SEM image of iron-rich cements formed in treated samples from T1, in which only the electric current was
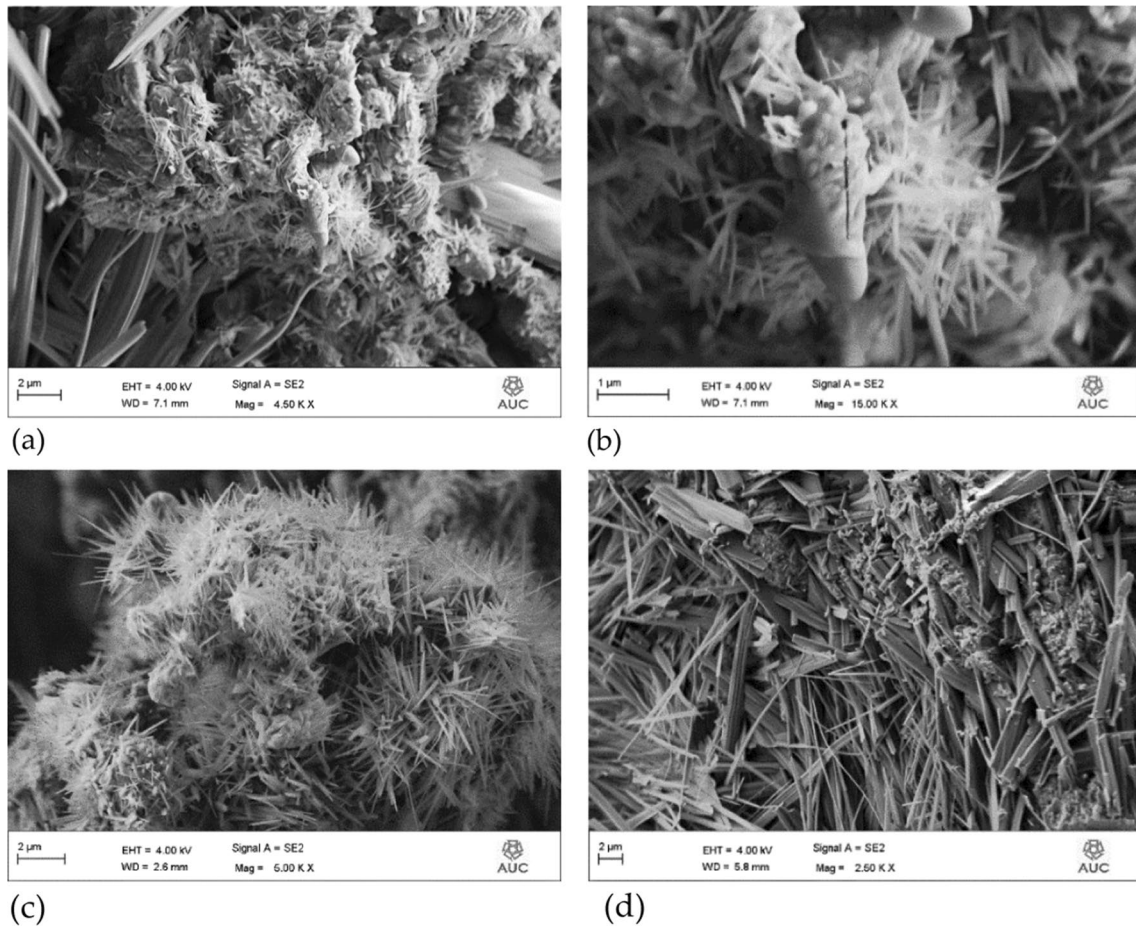
Fig. 15 Various microstructures of C–S–Hs grown in treated sand samples from T5 (iron electrodes) including **a** nodules at Mag 4.5 K, **b** nodules at Mag 15 K, **c** needle form and **d** rods
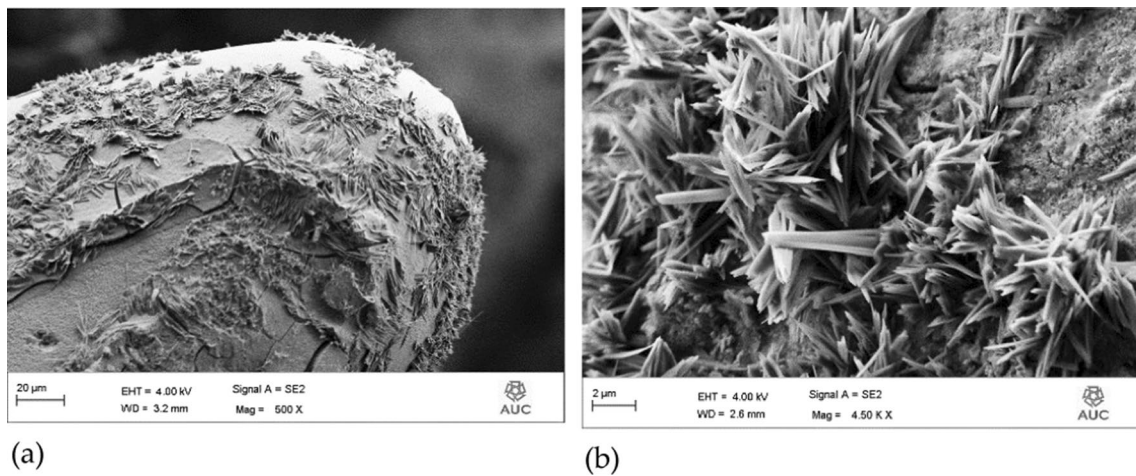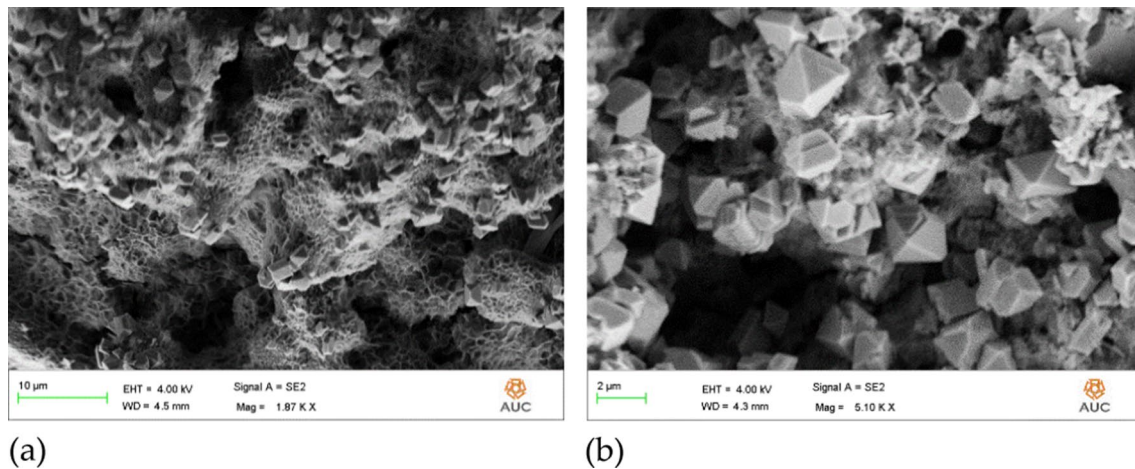

Fig. 16 SEM image showing the growth of C–S–H **a** on surface of individual sand grains and **b** between sand grains

passed through the calcareous sand without adding any chemical stabilisers, is shown in Fig. 12.
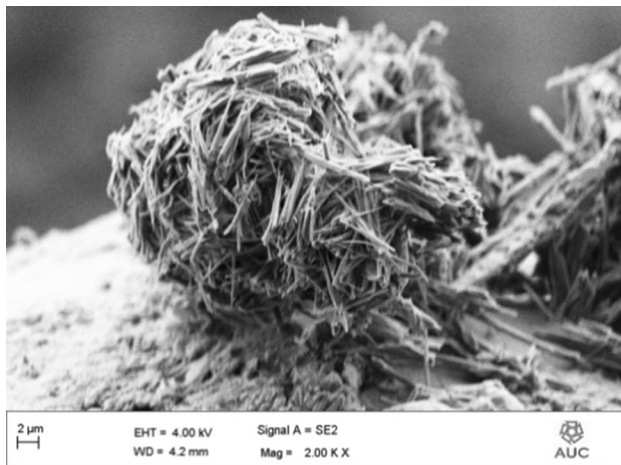
In addition to the iron oxides precipitated in the soil due to the corrosion of stainless-steel electrodes, other elements present in the alloy including chromium, nickel

Fig. 17 SEM image showing the growth of tobermorite in samples from T8

and magnesium were detected by EDX and EDX mapping of the treated sand samples. Sulphur is also naturally present in stainless steel and sometimes added to enhance the properties of the alloy. It is usually bonded in the form of manganese sulphides. The presence of this non-metallic element was also confirmed by EDX and EDX mapping of the treated sand. The above-mentioned alloying elements resulted in the formation of additional minerals in the treated calcareous sand like calcium magnesium carbonate $[(Ca, Mg)(CO_3)]$ and gypsum $(CaSO_4 \cdot 2H_2O)$ as revealed by XRD analysis of the treated samples.

Crystalline plates of Portlandite $[Ca(OH)_2]$ and C–S–Hs detected in a sample from T5 are shown in the SEM image in Fig. 13. SiO_2 nanoparticles reacted with $Ca(OH)_2$ and formed C–S–Hs in the form of tobermorite gel $(C_3S_2H_3)$, dicalcium silicate (C_2S) and tricalcium silicate (C_3S), which

are the main strength-contributing components of the pozzolanic activity. The pozzolanic reactions created various compounds and gels and caused alterations in the microstructure of the treated sand and resulted in its hardness. The microstructures of the treated sand samples were assessed for long-term reactions. Calcium hydroxide and silicon oxide were the feedstocks for pozzolanic reactions. Consequently, the increase in CS percent weight in the mix caused the pores between sand particles to be filled with more cementitious compounds and hence, resulted in more pronounced flocculation structures. Thus, the compressive strength increased as the percentage weight of CS increased.

Self-oriented rosettes of C–S–Hs grown in treated sand samples from T5 (in which iron electrodes were used instead of stainless steel) are shown in Fig. 14. In addition, Fig. 15a–d shows SEM images displaying various microstructures of C–S–Hs formed within samples from T5, including nodules, needle form and rods of C–S–Hs.

The presence of alumina powder (Al_2O_3) further contributed to the strength gain through the formation of aluminates with the end-product, ettringite $(3CaO \cdot Al_2O_3 \cdot 3CaSO_4)$. The SEM images of the treated sand samples from T8 are presented in Figs. 15, 16, 17, 18, 19 and 20, showing the microstructural developments in the matrix of the electrochemically stabilised calcareous sand as a result of the synergistic effect of the two pozzolans, CS nanoparticles and alumina powder.

The microstructural analyses of samples from T8 manifested cementation of the samples and the various minerals behind that. The SEM images showed diverse polymorphisms. SEM images show the growth of C–S–Hs and C-A-Hs on the surface of individual sand grains, as well as between grains, as displayed in Fig. 16a and b, respectively.

Crystalline calcium silicate hydrate (C–S–H) phases arise in the microstructure of the treated sand samples.

Fig. 18 Alpha-dicalcium silicate hydrate (hillebrandite), α-C_2SH ($Ca_2[HSiO_4](OH)$), detected by **a** SEM imaging and **b** XRD analysis

(a)   (b)

Fig. 19 SEM images of octahedral hydrogarnet and honeycomb structures of C–S–Hs detected in sample containing 1% alumina from T8 at Mag **a** 1.87 K and **b** 5.1 K

Fig. 20 SEM image of calcium aluminate, possibly pleochroite, formed on the surface of a sand grain in T8

Amorphous tobermorite gel ($3CaO\ 2SiO_2.3H_2O$) is shown in Fig. 17. Alpha-dicalcium silicate hydrate, hillebrandite, α-C_2SH ($Ca_2[HSiO_4](OH)$) are detected in SEM images and confirmed by XRD analysis, as shown in Fig. 18a and b, respectively. Octahedral hydrogarnet, $Ca_3Al_2(OH)_{12}$-$Ca_3Al_2Si(OH)_8$, was detected along with honeycomb structures of C–S–Hs as displayed in Fig. 19a and b.

SEM image of calcium aluminate, possibly pleochroite, is shown in Fig. 20. Rigid needle-like crystals of hydrous calcium aluminium sulphate (AFT), known as ettringite [$3CaO\cdot Al_2O_3\cdot 3CaSO_4\cdot 32H_2O$], were detected in the treated samples, as shown in Fig. 21.

Conclusions

Electro-cementation of calcareous sand containing 95.3% calcium carbonate was investigated through a series of laboratory experiments. Chemical stabilisers were added to the sand and a DC current was applied to the mix in an electrokinetic (EK) cell. Agents added to the sand were CS nanoparticles and alumina powder as 10%, 15%, 20%, 25% and 1% by weight of sand, respectively, to study the single effect of CS and the hybrid effect of the two stabilisers.

Compressive strength tests were performed on the treated sand samples. Spectroscopic analyses including FE-SEM, EDX and XRD were carried out to further assess the electro-cementation of the treated samples.

The following conclusions can be drawn from the results of the study:

1. The method resulted in the electro-cementation of the calcareous sand through the formation of calcium silicate hydrates (C–S–Hs) and calcium aluminate hydrates (C-A-Hs) within the structure of the treated sand samples. The newly formed compounds are the result of electrochemical reactions including electrolysis, redox as well as pozzolanic reactions which extended beyond the treatment period. The new mineral formation was confirmed by spectroscopic analyses including FE-SEM, XRD and EDX.

2. The treatment can be considered an artificial lithification process through which the treated soil was altered from a granular material into a rock similar to siliceous limestone with respect to its chemical structure. According to rock classification based on compressive strength, the resulting formation is a weak rock.
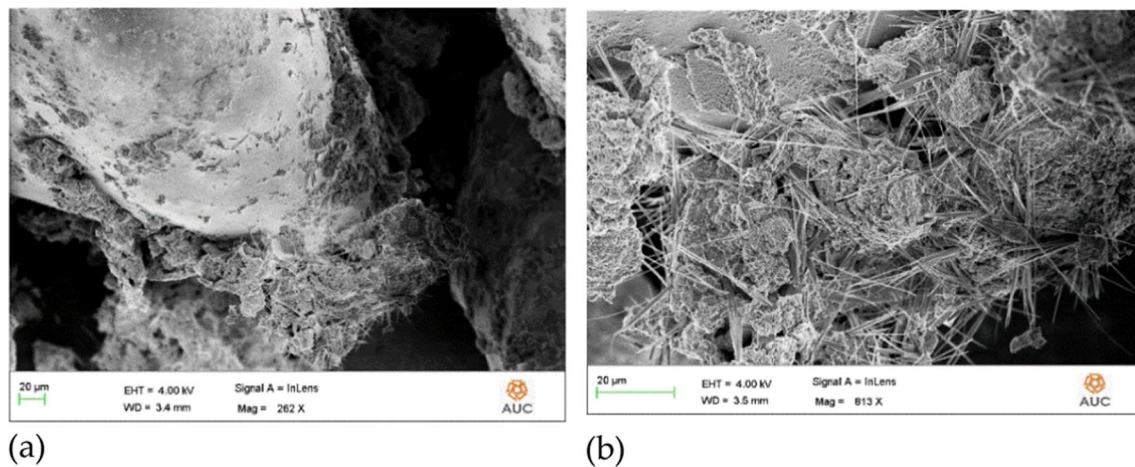
Fig. 21 SEM image of ettringites (AFT) and C–S–Hs formed on sand grains of treated sample from T8 at Mag **a** 262 and **b** 813

3. Hardening was not achieved immediately upon the completion of the treatment after the disconnection of the electric current but rather takes place due to pozzolanic reactions which extend beyond the treatment time. The treated sand samples were left in the EK cell for sixty days before sample extraction.

4. The application of the EK treatment without adding any chemical stabilisers brought about minor improvement in the compressive strength of the treated sand samples.

5. The addition of CS nanoparticles significantly improved the compressive strength of the treated sand samples. The compressive strength is enhanced by 20%, 60%, 171% and 167% due to the addition of 10%, 15%, 20% and 25% CS, respectively.

6. The improvement of compressive strength is directly proportional to the percent weight of CS nanoparticles. However, the optimum percent weight is 20%. Upon the addition of 25% CS, the improvement in compressive strength starts to decline.

7. The addition of alumina powder further contributed to the improvement brought about in the compressive strength. The use of nanosilica and alumina powder in a binary combination enhances the mechanical properties of the treated sand and is largely dependent on the silica/alumina ratio in the mix. The unconfined compressive strength and the modulus of elasticity increased by 133% and 113%, respectively, in the presence of 10% CS, and by 11% and 34%, respectively, in the presence of 20% CS.

8. The incorporation of 1% Al_2O_3 is almost equivalent to the incorporation of 10% CS. Nevertheless, the hybrid effect of the two pozzolans together should not be neglected.

9. The results obtained from using iron plate electrodes were like those obtained from using stainless-steel plate electrodes.

10. There were some limitations related to the process operation including the following. The current intensity decreases for the same applied voltage due to soil resistivity and concentration polarisation. This makes the electric field distribution difficult to study as the relation between the applied voltage and the current intensity becomes nonlinear. Also, the heat generated from the EK process causes a loss of soil-electrode contact making the treatment less effective and may lead to a premature termination of the process. The way to overcome this problem is to increase the applied voltage to maintain the current intensity, which leads to higher power consumption.

11. The treatment is successful in stabilising calcareous sand, and the technique has high potential for field applications, including caissons, highway construction projects, dune fixation and erosion control. The method can also be used for liquefaction mitigation due to electrolysis of pore water and its conversion into gases evolving at the anode and the cathode in addition to filling the pores with cementitious materials.

12. Further research is needed to test the efficiency of the treatment using the binary effect of CS and alumina powder at different contents of alumina powder above 1%.

Declarations

Conflict of interest The authors declare that they have no conflict of interest.

Ethical approval The article does not contain any studies with human participants or animals performed by any of the authors.

References

1. Pando MA, Sandoval EA, Catano J (2012) Liquefaction susceptibility and dynamic properties of calcareous sands. In: 15th world conference on earthquake engineering, Puerto Rico
2. Smith DA, Cheung KF (2003) Settling characteristics of calcareous sand. Hydraul Eng 129(6):479–483. https://doi.org/10.1061/(ASCE)0733-9429(2003)129:6(479)
3. McDowell GR, Bolton MD (2000) Effect of particle size distribution on pile tip resistance in calcareous sand in the geotechnical centrifuge. Granular Matter 2:179–187
4. Ata A, Salem TN, Hassan R (2018) Geotechnical characterization of the calcareous sand in northern coast of Egypt. Ain Shams Eng 9:3381–3390
5. Mohamedelhassan E, Shang JQ, Ismail MA, Randolph MF (2005) Electrochemical cementation of calcareous sand for offshore foundations. Offshore Polar Eng 15(1):71–79
6. Iqbal Khan M (2018) Nanosilica/silica fume. Waste Suppl Cem Mater Concr. https://doi.org/10.1016/B978-0-08-102156-9.00014-6
7. Bahmani SH, Bujang BK, Asadi A, Farzadnia N (2014) Stabilization of residual soil using SiO$_2$ nanoparticles and cement. Constr Build Mater 64:350–359
8. Malekzadeh M, Lovisa J, Sivakugan N (2016) An overview of electrokinetic consolidation of soils. Geotech Geol Eng 34:759–776. https://doi.org/10.1007/s10706-016-0002-1
9. Lee JK, Shang JQ (2014) Electrochemical stabilization of offshore and onshore soils: a review. The International Society of Offshore and Polar Engineers. ISBN 978-1 880653 91–3; ISSN 1098–6189
10. Rittirong A, Shang JQ, Mohamedelhassan E, AIsmail MF, Randolph M (2007) Effect of electric field intensity on electro-cementation of caissons in calcareous sand. Offshore and Polar Engineering 17(1):74–79
11. Rittirong A, Shang JQ, Mohamedelhassan E, AIsmail MF, Randolph M (2008) Effects of electrode configuration on electrokinetic stabilization for caisson anchors in calcareous sand. Geotech Geoenviron Eng. https://doi.org/10.1061/(ASCE)1090-0241(2008)134:3(352)
12. Nozari MA, Ziaie Moayed R, Amirkabir J (2019) Feasibility study of coupled hydraulic and electrophoretic injecting colloidal silica in sand. Civil Eng 51(2):87–89. https://doi.org/10.22060/ceej.2018.13408.5403
13. Darab B, Naeini SA, Nozari MA (2022) Effect of electrokinetic method on improvement of loose sand by colloidal silica. Arab J Geosci 15:302
14. Wang Y, Li A, Cui C (2021) Remediation of heavy metal-contaminated soils by electrokinetic technology: mechanisms and applicability. Chemosphere 265:129071
15. ASTM D422–63 Standard test method for particle-size analysis of soils
16. ASTM D4253 Standard test methods for maximum index density and unit weight of soils using a vibratory table
17. ASTM D4254–16. Standard test methods for minimum index density and unit weight of soils and calculation of relative density
18. Hallsworth CR, Knox R (1999) Rock classification scheme. Volume 3, classification of sediments and sedimentary rocks. Keyworth, Nottingham, British Geological Survey, pp 24
19. ASTM D1557. Standard Test Methods for Laboratory Compaction Characteristics of Soil Using Modified Effort
20. Zhang X, Yang H, Yang Q, Du X (2019) Effects of particle size of colloidal nanosilica on hydration of Portland cement at early age. Adv Mech Eng 11(2):1–9. https://doi.org/10.1177/1687814019828948
21. Gallagher PM, Mitchell JK (2002) Influence of colloidal silica grout on liquefaction potential and cyclic undrained behavior of loose sand. Soil Dyn Earthq Eng 22:1017–1026
22. Huang Y, Wang L (2016) Experimental studies on nanomaterials for soil improvement: a review. Environ Earth Sci 75:497. https://doi.org/10.1007/s12665-015-5118-8
23. Al-maamori MH, Ahmed JK, Ali HM (2015) Production of nano-silica from water glass. Acad Res Int 6(1):2223–9944
24. Ramezanianpour AA, Mortezaei M, Mirvalad S (2021) Synergic effect of nano-silica and natural pozzolans on transport and mechanical properties of blended cement mortars. Build Eng. https://doi.org/10.1016/j.jobe.2021.102667
25. Tsai MS, Huang PY, Yang CH (2006) Formation mechanisms of colloidal silica via sodium silicate. Nanoparticle Res 8:943–949. https://doi.org/10.1007/s11051-005-9047-4
26. Gidudu B, Chirwa EMN (2022) The role of pH, electrodes, surfactants, and electrolytes in electrokinetic remediation of contaminated soil. Molecules 27:7381. https://doi.org/10.3390/molecules27217381
27. Glendinning S, Jones CJFP, Lamont-Black J (2005) The use of electrokinetic geosynthetics (EKG) to improve soft soils. Geo Eng Book Ser. https://doi.org/10.1016/S1571-9960(05)80038-2
28. Mohamedelhassan E, Shang JQ (2001) Effects of electrode materials and current intermittence in electro-osmosis. Proc Inst Civ Eng Ground Improv 5(1):3–11. https://doi.org/10.1680/grim.5.1.3.39435
29. Hencher S (2015) Practical rock mechanics. Taylor and Francis
30. Alfreds RJ (1979) Rock mechanics. Trans Tech Publications
31. Jackson RE (2019) Earth science. Cambridge University Press
32. Neville AM, Brooks JJ (2019) Concrete technology. Pearson
33. Sachin R (2016) Concrete technology. S.K. Kataria and Sons